



PERGAMON

Available online at [www.sciencedirect.com](http://www.sciencedirect.com)

SCIENCE @ DIRECT®

Polyhedron 22 (2003) 2343–2348



POLYHEDRON

[www.elsevier.com/locate/poly](http://www.elsevier.com/locate/poly)

# Magnetism in organic radical ion salts based on nitronyl nitroxide derivatives substituted with heterocyclic aromatic hydrocarbons

Tadashi Sugano<sup>a,b,\*</sup>, Stephen J. Blundell<sup>b</sup>, William Hayes<sup>b</sup>, Peter Day<sup>c</sup>

<sup>a</sup> Department of Chemistry, Meiji Gakuin University, Kamikurata, Totsuka-ku, Yokohama 244-8539, Japan

<sup>b</sup> Department of Physics, Clarendon Laboratory, University of Oxford, Parks Road, Oxford OX1 3PU, UK

<sup>c</sup> Royal Institution of Great Britain, 21 Albemarle Street, London W1S 4BS, UK

Received 8 October 2002; accepted 3 March 2003

## Abstract

Radical cation and anion salts of the neutral organic radicals, 2-imidazolyl nitronyl nitroxide (2-IMNN) and 2-benzimidazolyl nitronyl nitroxide (2-BIMNN), have been prepared and their magnetic properties studied by SQUID magnetometry. The radical salts exhibit one-dimensional (1-d) antiferromagnetic (AFM) intermolecular interactions with the exchange coupling  $J/k$  between  $-0.8$  and  $-6.3$  K, which are significantly reduced from those observed in the two neutral radicals, while 2-IMNN shows an AFM interaction with  $J/k = -88$  K within the molecular dimers and 2-BIMNN has quasi 1-d ferromagnetic (FM) intermolecular interactions with  $J/k = +22$  K (intrachain) and  $zJ'/k = +0.24$  K (interchain). The magnetic properties of the nitronyl nitroxide and iminonitroxide derivatives having molecular structure related to 2-IMNN have also been investigated. In 2-benzimidazolyl iminonitroxide (2-BIMIN), the FM interaction observed in 2-BIMNN is replaced by strong 1-d AFM interaction with  $J/k = -11.7$  K.

© 2003 Elsevier Science Ltd. All rights reserved.

**Keywords:** Nitronyl nitroxide; Radical ions; Magnetism; Organic crystals; Ionic crystals

## 1. Introduction

Introducing ionic character into organic radical nitronyl nitroxide (2-substituted 4,4,5,5-tetramethyl-4,5-dihydro-3-oxido-1*H*-imidazol-3-ium-1-yl-oxyl) derivatives by making radical ions is of interest in extending the field of organic magnetism, because the ionic character may yield ionic crystals of the nitronyl nitroxide radicals, which sometimes give ferromagnetic (FM) intermolecular interactions [1–3]. Nitronyl nitroxide is usually obtained as a stable neutral radical. However, it can be transformed into various ionic states as shown in Fig. 1. Diradical cations could be obtained by eliminating an electron from the substituted moiety of the radical [4,5], while diradical anions are possible by

adding an electron. On the other hand, radical cations could be prepared by adding a proton or an alkyl cation into the substituted moiety [6], while elimination of a proton yields radical anions [7,8].

When the substituted nitronyl nitroxide moiety has the character of an electron donor or acceptor, an electron transfer out of a donating or into an accepting moiety may yield a charge-transfer (CT) salt (or complex) by combining it with an acceptor or donor molecule, respectively, as shown in Fig. 1. In this case, a complete (one electron) CT results in a diradical cation or diradical anion of nitronyl nitroxide. Regardless of molecular stacking patterns in the crystals, the CT salts and complexes, which include additional spin centers on the radical moieties with respect to conventional donor–acceptor type CT salts and complexes, may give three-spin interacting systems and could therefore result in a ferrimagnetic state when the FM interaction between the spins both on the nitronyl nitroxide molecule is strong enough to maintain the spins parallel. When the CT

\* Corresponding author. Tel.: +81-45-863-2122; fax: +81-45-863-2124.

E-mail address: [sugano@mail.meijigakuin.ac.jp](mailto:sugano@mail.meijigakuin.ac.jp) (T. Sugano).

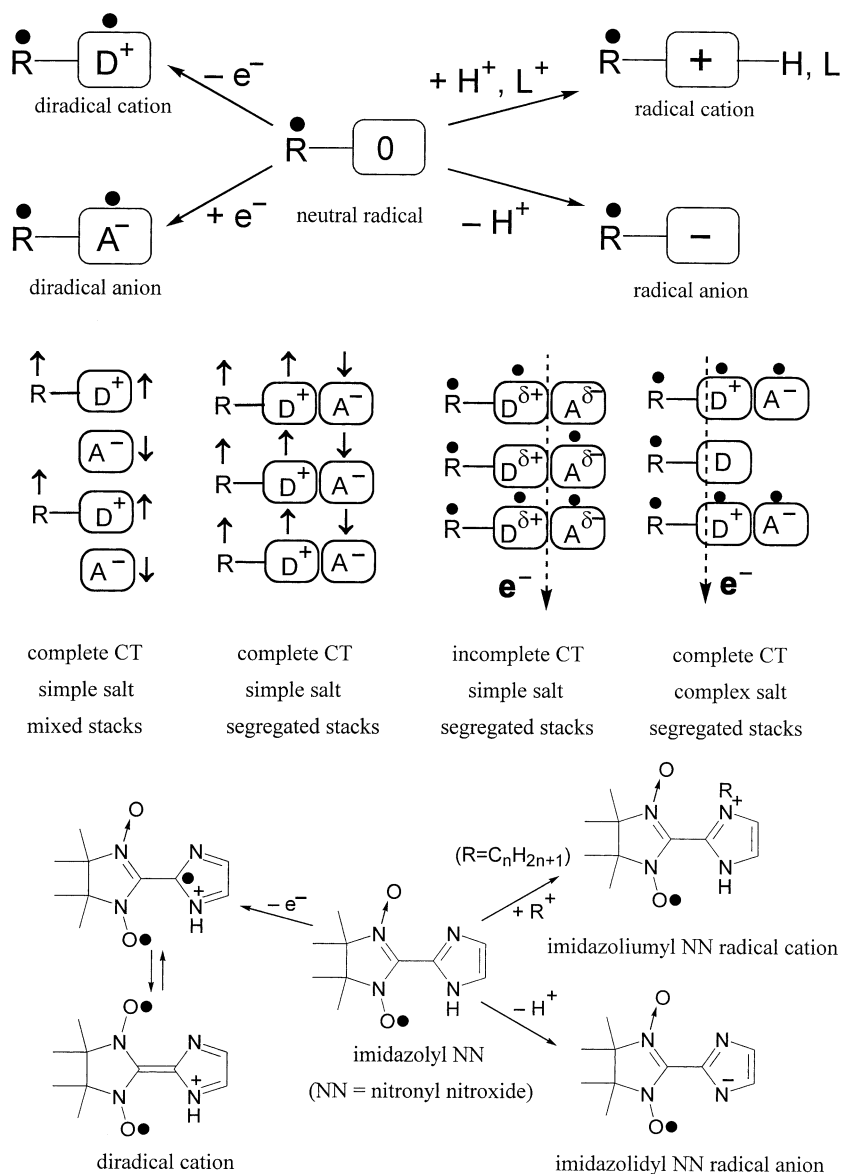


Fig. 1. A schematic view of multi-functional character of a nitronyl nitroxide derivative having the molecular moiety that has a potential of electron and/or proton transfer. The round-corner rectangle represents the substituent moiety. R represents the nitronyl nitroxide radical moiety and L indicates an alkyl group. The dots indicate unpaired electrons and the short arrows represent their spins. The dashed long arrow represents a conducting path. At the bottom a multi-functional character of 2-IMNN is shown.

salts and complexes crystallize in segregated stacks and also are complex salts or in incomplete CT states, as observed in the organic complex tetrathiafulvalene–tetracyanoquinodimethane (TTF–TCNQ), there could be magnetic interactions between conduction-electron spins and localized-electron spins as shown in Fig. 1.

To obtain ionic nitronyl nitroxide derivatives mentioned above, we have been preparing and studying physical properties of the nitronyl nitroxide having dialkylaminophenyl, imidazolyl, carboxyaryl and sulfoaryl substituents [4,8–12]. Carboxyaryl and sulfoaryl groups easily lose a proton, leaving carboxylate and sulfonate anions, so that the nitronyl nitroxide derivatives having these moieties give radical anions. Of these

substituents, the imidazolyl group is the most interesting one because it may yield many different kinds of ions from the same molecule, as shown in Fig. 1. We have therefore prepared radical ion salts and complexes of the two neutral derivatives of imidazolyl nitronyl nitroxide; 2-imidazolyl nitronyl nitroxide (2-IMNN) [8,9,13] and 2-benzimidazolyl nitronyl nitroxide (2-BIMNN) [14].

In this paper, we present magnetic properties of radical cation and anion salts of 2-IMNN and 2-BIMNN. In addition, to discuss the effects of hydrogen-bonds on the magnetic properties of these two radicals, the magnetic behavior of the neutral radicals, 2-benzimidazolyl iminonitroxide (2-BIMIN), 2-thiazolyl nitronyl nitroxide (2-TAZNN) and 2-pyrrolyl nitronyl

nitroxide (2-PRNN), having molecular structures close to the imidazolyl derivatives, is also described.

## 2. Experimental

The radicals, of which molecular structures are shown in Fig. 2, were prepared according to the procedures reported elsewhere [15,16]. The radical anion salts were prepared through the reaction between the neutral radical and sodium hydroxide or tetrabutylammonium hydroxide in a methanol solution. The radical cation salts were prepared by reacting the radicals in iodomethane. The magnetization isotherms up to 7 T and magnetic susceptibility over the temperature range from 1.8 to 300 K was measured by using Quantum Design MPMS and MPMSXL7 SQUID (superconducting quantum interference device) magnetometers. The contribution of the diamagnetism to the susceptibility was subtracted by extrapolating the temperature dependence of susceptibility to high temperatures where the Curie–Weiss law is applicable.

## 3. Results and discussion

Figs. 3 and 4 show the temperature dependence of the product of paramagnetic susceptibility  $\chi_p$  and temperature  $T$  of 2-IMNN, 2-BIMNN and 2-BIMIN. Upon lowering the temperature, the product,  $\chi_p T$ , of 2-BIMNN increases steeply below 10 K as shown in Fig. 3, while that of 2-IMNN decreases rapidly below 200 K toward almost zero at temperatures lower than 20 K as shown in Fig. 4. Note the different scales of  $\chi_p T$  between Figs. 3 and 4.

The  $\chi_p T$  value of 2-BIMNN increases up to 5.44 emu K mol<sup>-1</sup> at 1.82 K, which was the lowest temperature available in our measurements. This value is 15 times as high as 0.376 emu K mol<sup>-1</sup>, expected for  $S = 1/2$  non-interacting spin systems, thereby indicating a remark-

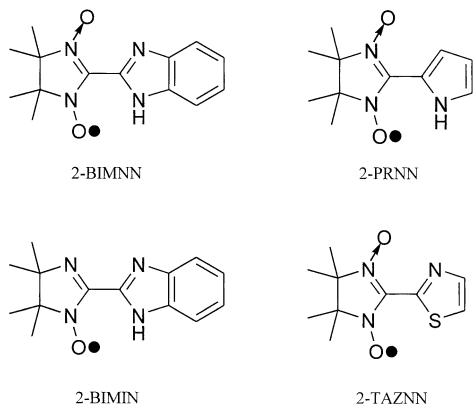


Fig. 2. Molecular structures of organic radicals.

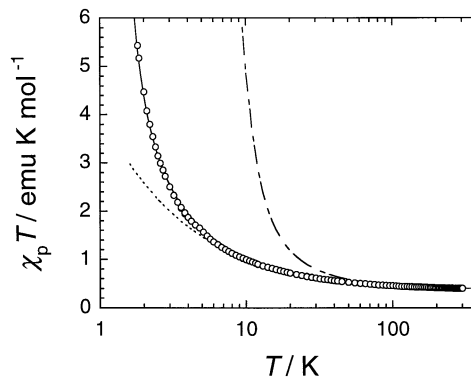


Fig. 3. Temperature dependence of  $\chi_p T$  of 2-BIMNN. Open circles represent experimental data. Solid line indicates theoretical fitting on the basis of the quasi 1-d FM Heisenberg model (see the text). Broken and dashed lines show theoretical fittings based on the 1-d FM Heisenberg model and 2-d FM square-lattice model, respectively.

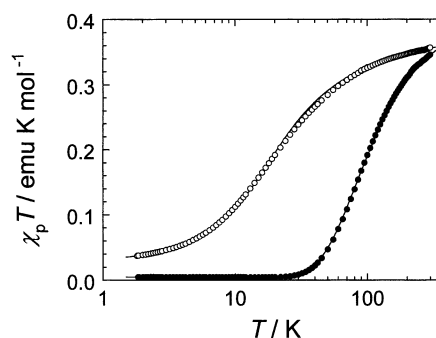


Fig. 4. Temperature dependence of  $\chi_p T$  of 2-IMNN and 2-BIMIN. Closed and open circles represent experimental data for 2-IMNN and 3-BIMIN, respectively. Each solid line indicates theoretical fitting on the basis of the dimer (2-spin) model for 2-IMNN and the 1-d AFM Heisenberg model for 2-BIMIN.

ably strong FM intermolecular interaction. In contrast to the results reported in Ref. [14], the  $\chi_p T$  value of 2-BIMNN does not exhibit any maximum around 3 K and increases monotonically down to 1.82 K. The maximum appears to be the result of saturation in magnetization under high magnetic field at low temperatures. We thus measured magnetic susceptibility under 20 mT below 10 K to avoid the effects of saturation.

Above 10 K the temperature dependence of  $\chi_p T$  of 2-BIMNN is modeled by the one-dimensional (1-d) FM Heisenberg model [17] with  $J/k = +22$  K, where  $J$  is the exchange coupling constant with the spin Hamiltonian  $\mathcal{H} = \min 2J \sum S_i S_j$  and  $k$  the Boltzmann constant, as shown by the dotted line in Fig. 3. The data can be fitted by the Curie–Weiss law only above 70 K with the Weiss constant  $\theta = +17$  K (not shown), while the two-dimensional (2-d) FM square-lattice model [18] does not give good fits below 50 K, as shown by the dash-dotted line in Fig. 3. Below 5 K, however, the experimental data deviate toward larger values from those of  $\chi_p^{1d} T$  calculated by using the 1-d FM model with decreasing

temperature. This discrepancy is successfully interpreted by introducing FM interactions between the 1-d FM chains. By using the expression  $\chi_p T = \chi_p^{\text{ld}} T [1 - 2zJ^{\text{ld}} \chi_p^{\text{ld}} / Ng^2 \mu_B^2]^{-1}$  on the basis of the mean-field theory [19], the temperature dependence of  $\chi_p T$  is reproduced well with the FM interchain coupling  $zJ/k = +0.24$  K, where  $z$  is the number of neighboring chains and  $J$  the interchain exchange coupling constant, over the whole temperature range examined, as shown by the solid line in Fig. 3. The results mentioned above clearly suggest that 2-BIMNN is a strongly anisotropic quasi 1-d FM radical crystal with  $J/J' = 25 \sim 50$ .

In 2-IMNN,  $\chi_p T$  decreases down to almost zero as the temperature decreases. This behavior suggests an antiferromagnetic (AFM) intermolecular interaction. The experimental data are well reproduced by the dimer (2-spin) model [20] with  $J/k = -88$  K as shown by the solid line in Fig. 4. The magnitude of the AFM interaction obtained for 2-IMNN is significantly strong for nitronyl nitroxide derivatives and compared with that observed in the radical cation salt 1-methylpyridinium-4-yl nitronyl nitroxide iodide (*p*-MPYNN)<sup>+</sup>•I<sup>-</sup> ( $J/k = -74$  K) [21] and the low-temperature phase of 5-carboxy-2-thienyl nitronyl nitroxide (2-CATNN) ( $J/k = -48$  K) [22], whereas many nitronyl nitroxide radicals give  $J/k$  values less than 10 K [1–3]. It is therefore, likely that imidazolyl derivatives of nitronyl nitroxide have a potential to yield strong intermolecular interactions both in FM and AFM.

In 2-BIMIN, of which molecular structure is close to 2-BIMNN as shown in Fig. 2,  $\chi_p T$  decreases gradually as the temperature decreases, in contrast to the remarkably steep increase observed in 2-BIMNN. This result suggests that the oxygen atoms on the NO groups play an essential role in determining the sign and magnitude of magnetic interactions. In the crystal, the 2-BIMNN molecules form 1-d molecular stacking arrangements through hydrogen-bonds between the hydrogen atoms on the imidazol rings and the oxygen atoms on the nitronyl nitroxide moieties [14]. Although the molecular arrangement of 2-BIMIN in the crystal is not known at present, the experimental data are interpreted by using the 1-d AFM Heisenberg model [23] with  $J/k = -11.7$  K. Therefore, the 1-d interaction remains in 2-BIMIN, whereas the FM interaction has disappeared. To acquire further insight into the magneto-structural correlation in the two nitronyl nitroxide derivatives, crystal structure analysis of 2-BIMIN is indispensable.

Fig. 5 shows the temperature dependence of  $\chi_p T$  of the radical cation salt 3-methylbenzimidazolium-2-yl nitronyl nitroxide (2-MBIMNN)<sup>+</sup>•I<sup>-</sup>, and the anion radical salts sodium 2-benzimidazolidyl nitronyl nitroxide Na<sup>+</sup>(2-BIMNN)<sup>-</sup>• and tetrabutylammonium 2-benzimidazolidyl nitronyl nitroxide (TBA)<sup>+</sup>(2-BIMNN)<sup>-</sup>•. In contrast to the neutral radical 2-BIMNN, all the salts exhibit AFM intermolecular

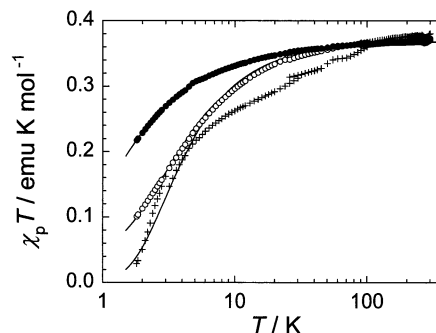


Fig. 5. Temperature dependence of  $\chi_p T$  of (2-MBIMNN)<sup>+</sup>•I<sup>-</sup>, Na<sup>+</sup>(2-BIMNN)<sup>-</sup>• and (TBA)<sup>+</sup>(2-BIMNN)<sup>-</sup>• shown by crosses, open circles and closed circles, respectively. Theoretical fitting for each compound is represented by a solid line.

interactions. Although it is difficult to fit the experimental data over the whole temperature range, magnetic behavior of the cation radical salt (2-MBIMNN)<sup>+</sup>•I<sup>-</sup> can be analyzed on the basis of the dimer model, described for 2-IMNN, with  $J/k = -3.2$  K.

The temperature dependence of  $\chi_p T$  of Na<sup>+</sup>(2-BIMNN)<sup>-</sup>• is reproduced well by using the 1-d AFM Heisenberg model with  $J/k = -1.95$  K. The temperature dependence of  $\chi_p$  of this salt shows a maximum at 2.3 K. In the  $S = 1/2$  1-d AFM Heisenberg model, the maximum of  $\chi_p$  is located at  $1.282 J/k$  [24]. This relation gives a maximum at 2.50 K, which is close to the experimental findings. The temperature dependence of  $\chi_p T$  of (TBA)<sup>+</sup>(2-BIMNN)<sup>-</sup>• is also interpreted by the 1-d AFM Heisenberg model with  $J/k = -0.80$  K. In this case, the maximum of  $\chi_p$  is expected at 1.02 K, which is lower than the lowest temperature available to us. The experimental data of (TBA)<sup>+</sup>(2-BIMNN)<sup>-</sup>• can be explained by the Curie–Weiss law with  $\theta = -1.11$  K. However, the calculated values deviate positively from the experimental data below 3 K. In summary, the two radical anion salts of 2-BIMNN exhibit 1-d AFM behavior, while the radical cation salt of 2-BIMNN shows behavior characteristic of the isolated AFM dimer. In none of the salts is the FM behavior observed in 2-BIMNN.

Fig. 6 shows the temperature dependence of  $\chi_p T$  of the radical cation salt 3-methylimidazolium-2-yl nitronyl nitroxide (2-MIMNN)<sup>+</sup>•I<sup>-</sup>, and the anion radical salts sodium 2-imidazolidyl nitronyl nitroxide Na<sup>+</sup>(2-IMNN)<sup>-</sup>• and tetrabutylammonium 2-imidazolidyl nitronyl nitroxide (TBA)<sup>+</sup>(2-IMNN)<sup>-</sup>•. The temperature dependence of  $\chi_p T$  of Na<sup>+</sup>(2-IMNN)<sup>-</sup>• is reproduced well by the 1-d AFM Heisenberg model with  $J/k = -6.3$  K, as shown by the solid line in Fig. 6. The temperature dependence of  $\chi_p$  of this salt shows a maximum at 7.0 K, which is close to 8.1 K calculated by the relation mentioned above.

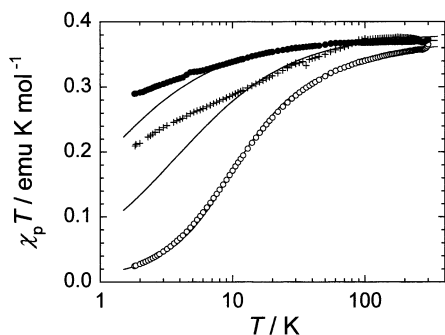


Fig. 6. Temperature dependence of  $\chi_p T$  of  $(2\text{-MIMNN})^+ \cdot \text{I}^-$ ,  $\text{Na}^+(2\text{-IMNN})^- \cdot$  and  $(\text{TBA})^+(2\text{-IMNN})^- \cdot$  shown by crosses, open circles and closed circles, respectively. Theoretical fitting for each compound is represented by a solid line.

The temperature dependence of  $\chi_p T$  of  $(2\text{-MIMNN})^+ \cdot \text{I}^-$  and  $(\text{TBA})^+(2\text{-IMNN})^- \cdot$  is not interpreted in terms of any models discussed here over the whole temperature range measured as shown by the solid lines in Fig. 6. Above 15 K, the experimental data of  $(2\text{-MIMNN})^+ \cdot \text{I}^-$  are fitted to the Curie–Weiss law with  $\theta = -3.7$  K. Below 10 K, however, the experimental data deviate toward larger values from those calculated by using the Curie–Weiss law with decreasing temperature. Similar behavior is observed in  $(\text{TBA})^+(2\text{-IMNN})^- \cdot$ . In this salt, the experimental data deviate from the Curie–Weiss law with  $\theta = -1.0$  K below 8 K. Since both the 1-d AFM Heisenberg model and the dimer model give more rapid decrease in  $\chi_p T$  at low temperatures compared with the Curie–Weiss law, these models could not explain the magnetic behavior, especially at low temperatures. These results are reminiscent of the coexistence of FM and AFM interactions [5,10].

Fig. 7 shows the temperature dependence of  $\chi_p T$  of 2-PRNN and 2-TAZNN having molecular structures relating to 2-IMNN as shown in Fig. 2. For comparison, the data for 2-IMNN are also shown. The nitrogen atom in 2-IMNN is replaced with a  $\geq \text{CH}$  group in 2-PRNN,

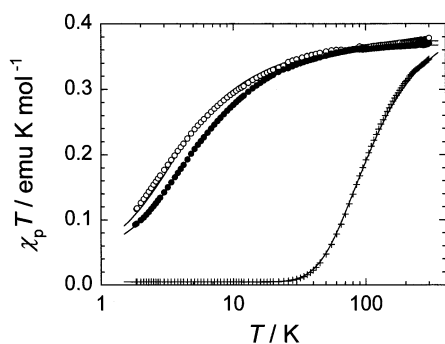


Fig. 7. Temperature dependence of  $\chi_p T$  of 2-TAZNN and 2-PRNN shown by open circles and closed circles, respectively. For comparison, the data for 2-IMNN are shown by crosses. Theoretical fitting for each compound is represented by a solid line.

while the  $> \text{NH}$  group in 2-IMNN is substituted by a sulfur atom in 2-TAZNN. These replacements could prevent the formation of the hydrogen-bonds which are observed in 2-IMNN [14], although the molecular size and shape are not so much different from each other.

The two neutral radicals 2-PRNN and 2-TAZNN show behavior similar to each other. The temperature dependences of  $\chi_p T$  of the two radicals are interpreted commonly in terms of the 1-d AFM Heisenberg model, as shown by the solid lines in Fig. 7. The exchange coupling  $J/k = -2.7$  K for 2-PRNN and  $-2.15$  K for 2-TAZNN. These values of exchange coupling are close to those obtained for the radical anion salts  $\text{Na}^+(2\text{-IMNN})^- \cdot$  ( $-6.3$  K),  $\text{Na}^+(2\text{-BIMNN})^- \cdot$  ( $-1.95$  K), and  $(\text{TBA})^+(2\text{-BIMNN})^- \cdot$  ( $-0.80$  K) and weaker than those observed in 2-BIMIN ( $-11.7$  K), 2-BIMNN ( $+22$  K) and 2-IMNN ( $-88$  K).

In the radical ion salts mentioned above, the counter ions may intercept hydrogen-bonds in the solids, as expected for the neutral radicals 2-PRNN and 2-TAZNN, which have lost the potential to form hydrogen-bonds. In contrast, the 2-BIMNN, 2-BIMNN and 2-IMNN molecules all have an imidazolyl rings that can form hydrogen-bonds between neighboring molecules. It is therefore likely that the hydrogen-bonds in these neutral radicals play an essential role in retaining strong intermolecular magnetic interactions.

In conclusion, we have shown that the strong intermolecular magnetic interactions observed in the (benz)imidazolyl derivatives of nitronyl nitroxide are significantly reduced by the introduction of counter ions in the solid forming their ion radical salts. It is likely that the counter ions intercept the hydrogen-bonds between neighboring imidazolyl rings. The replacements of the nitrogen atom or the  $> \text{NH}$  group in the imidazolyl ring by a  $\geq \text{CH}$  group or a sulfur atom, respectively, which reduce the potential to form the hydrogen-bonds, also reduce the intermolecular magnetic interactions. The elimination of the oxygen atom, which forms hydrogen-bonds with the imidazolyl ring in 2-BIMNN, on the nitronyl nitroxide moiety changes sign and reduces magnitude of intermolecular magnetic interaction. These results clearly suggest that the hydrogen-bonds through the imidazolyl rings of the nitronyl nitroxide derivatives are of crucial importance for obtaining strong intermolecular magnetic interactions.

## Acknowledgements

This work was in part carried out using facilities of the Institute for Solid State Physics, the University of Tokyo. The author is grateful to Professor Tajima for using the SQUID magnetometer.



## References

- [1] The papers published in *Mol. Cryst. Liq. Cryst.* 232 (1993), 271 (1995), 305 (1997), 334 (1999) and *Polyhedron*, 20 (2001).
- [2] K. Itoh, M. Kinoshita (Eds.), *Molecular Magnetism—New Magnetic Materials*, Kodansha Ltd/Gordon and Breach Science Publishers, Tokyo/Amsterdam, 2000.
- [3] D.B. Amabilino, J. Veciana, *Magnetism*, in: J.S. Miller, M. Drillon (Eds.), *Molecules to Materials II*, Wiley-VCH, Weinheim, 2001, p. 1.
- [4] T. Sugano, T. Fukasawa, M. Kinoshita, *Synth. Met.* 41–43 (1991) 3281.
- [5] T. Nakazaki, M.M. Matsushita, A. Izuoka, T. Sugawara, *Tetrahedron Lett.* 40 (1999) 5027.
- [6] K. Awaga, T. Inabe, Y. Maruyama, T. Nakamura, M. Matsumoto, *Chem. Phys. Lett.* 195 (1992) 21.
- [7] K. Inoue, H. Iwamura, *Chem. Phys. Lett.* 207 (1993) 551.
- [8] T. Sugano, M. Kurmoo, P. Day, *Synth. Met.* 85 (1997) 1729.
- [9] T. Sugano, S.J. Blundell, F.L. Pratt, W. Hayes, H. Uekusa, Y. Ohashi, M. Kurmoo, P. Day, *Mol. Cryst. Liq. Cryst.* 305 (1997) 435.
- [10] T. Sugano, P. Day, *Synth. Met.* 103 (1999) 2335.
- [11] T. Sugano, S.J. Blundell, F.L. Pratt, T. Jestädt, B.W. Lovett, W. Hayes, P. Day, *Mol. Cryst. Liq. Cryst.* 334 (1999) 477.
- [12] T. Sugano, S.J. Blundell, W. Hayes, P. Day, *Synth. Met.* 121 (2001) 1812.
- [13] N. Yoshioka, M. Irisawa, N. Aizawa, T. Aoki, H. Inoue, S. Ohba, *Mol. Cryst. Liq. Cryst.* 286 (1996) 165.
- [14] N. Yoshioka, M. Irisawa, Y. Mochizuki, T. Kato, H. Inoue, S. Ohba, *Chem. Lett.* (1997) 251.
- [15] E.F. Ullman, J.H. Osiecki, D.G.B. Boocock, R. Darcy, *J. Am. Chem. Soc.* 94 (1972) 7049.
- [16] K. Fegy, D. Luneau, T. Ohm, C. Paulsen, P. Rey, *Angew. Chem. Int. Ed.* 37 (1998) 1270.
- [17] G.A. Baker, Jr., G.S. Rushbrooke, H.E. Gilbert, *Phys. Rev.* 135 (1964) A1272.
- [18] G.A. Baker, Jr., H.E. Gilbert, J. Eve, G.S. Rushbrooke, *Phys. Rev.* 169 (1967) 800.
- [19] J.N. McElearney, D.B. Losee, S. Merchant, R.L. Carlin, *Phys. Rev. B* 7 (1973) 3314.
- [20] B. Bleaney, K.D. Bowers, *Proc. Roy. Soc. A* 214 (1952) 451.
- [21] K. Awaga, T. Inabe, U. Nagashima, T. Nakamura, M. Matsumoto, Y. Kawabata, Y. Maruyama, *Chem. Lett.* (1991) 1777.
- [22] T. Sugano, *Chem. Lett.* (2001) 32.
- [23] W.E. Hatfield, *J. Appl. Phys.* 52 (1981) 1985.
- [24] J.C. Bonner, M.E. Fisher, *Phys. Rev. A* 135 (1964) 640.